Indonesian Rainfall Variability: Impacts of ENSO and Local Air–Sea Interaction

HARRY H. HENDON

NOAA–CIRES Climate Diagnostics Center, Boulder, Colorado

(Manuscript received 9 November 2001, in final form 28 October 2002)

ABSTRACT

Relationships between Indonesian rainfall and Indo-Pacific sea surface temperatures (SSTs) and circulation anomalies are investigated using observations for 1951–97. Indonesia receives significant rainfall year-round but experiences a wet season that peaks in January and a dry season that peaks in August. Dry season rainfall anomalies are spatially coherent, strongly correlated with SST, and tightly coupled to El Niño–Southern Oscillation (ENSO) variations in the Pacific basin. Drought conditions typically occur during El Niño, when SSTs surrounding Indonesia are cool and the Walker circulation is weakened, resulting in anomalous surface easterlies across Indonesia. The opposite tends to occur during La Niña. Broadscale Indonesian rainfall and SST anomalies tend to not persist from the dry season into the wet season. Rainfall in the heart of the wet season tends to be uncorrelated with SST and spatially incoherent.

Seasonally varying feedback between Indonesian SST, winds, and rainfall explains the growth, persistence, and coherence of the local anomalies during the dry season and their decay or change in sign once the wet season commences. During the dry season anomalous surface easterlies, remotely driven by warm SSTs in the central Pacific during El Niño, act to increase local wind speed, cooling the ocean surrounding and to the east of Indonesia and thereby increasing the anomalous SST gradient across the Pacific. Hence, local rainfall and the Walker circulation are further reduced. Once the wet season commences and the climatological surface winds across Indonesia shift from southeasterly to northwesterly, the anomalous surface easterlies now act to reduce the wind speed. The initial cold SST anomaly is damped, reducing the negative rainfall anomalies and surface easterlies. The opposite scenario occurs during La Niña.

Indonesian rainfall variations during the dry season are also coupled to the development of an anomalous zonal SST gradient in the equatorial Indian Ocean. This anomalous gradient is strongly related to ENSO and is most prominent during the dry season. Once the wet season commences, the entire Indian Ocean tends to have the same-signed SST anomaly (positive during El Niño and negative during La Niña). Development and decay of this anomalous zonal SST gradient in the Indian Ocean is promoted by seasonally varying air–sea interaction in the eastern Indian Ocean in response to ENSO conditions in the Pacific. The eastern Indian Ocean SST changes are driven largely by induced surface heat flux variations (primarily changes in latent heat flux and net shortwave radiation). Biennial variations in the Indonesian region may also be induced by this seasonally varying air–sea interaction associated with ENSO.

1. Introduction

During the early stages of the 1997 El Niño,[1] drought conditions developed across Indonesia and much of the Maritime Continent (taken here to include the archipelagos of Indonesia, Malaysia, and New Guinea and the surrounding seas). Some locations in Indonesia experienced record air pollution and haze as a result of out of control forest and peat fires (Nichol 1998). Such haze episodes are not unprecedented: similarly poor conditions occurred during El Niño in 1994 (Nichol 1997). Fires are typically set during the dry half of the year (May–October), when land is cleared before planting. The onset of the wet season late in the year usually helps to contain and extinguish the fires. However, El Niño conditions can lead to disastrous consequences when early monsoon rainfall is delayed or reduced. Continued population growth in the region, with greater demands for croplands, suggests that such disasters will become more common in the future. This is emphasized by the fact the very strong El Niño of 1982 and the associated drought were accompanied by much weaker pollution and haze levels than in 1994 and 1997.

The severe environmental and societal consequences of untimely drought in Indonesia, together with the high sensitivity of extratropical circulation to variations in diabatic heating in this region (e.g., Ting and Sardeshmukh 1993), underscore the need to better understand

[1] El Niño in this study will refer to basinwide warm events in the Pacific, as opposed to its traditional usage to indicate warming off of the Peruvian coast. The basinwide warm events are not necessarily associated with coastal warming, but are associated with the Southern Oscillation and eastward shifts of convection into the central Pacific (e.g., Deser and Wallace 1990).

Corresponding author address: Harry Hendon, BMRC, P.O. Box 1289K, Melbourne 3001, Australia.
E-mail: h.hendon@bom.gov.au

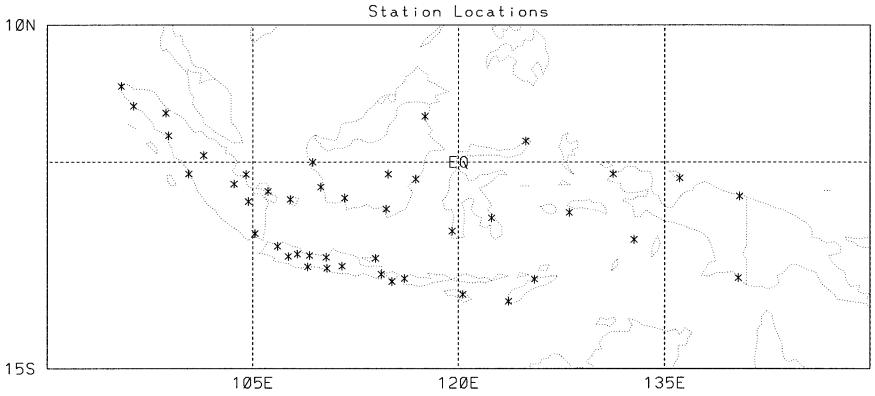

FIG. 1. Location of the 43 stations throughout Indonesia for which monthly rainfall records are available for the period 1951–97.

the nature and mechanisms of rainfall variability across the region. It has long been recognized that drought over the tropical west Pacific is associated with the low phase of the Southern Oscillation (e.g., Walker and Bliss 1932) and El Niño conditions in the Pacific (Bjerknes 1969). As such, drought in the Indonesian region is interpreted to result from remotely forced subsidence associated with an eastward shift of convection into the central Pacific and weakening of the Walker circulation. But, this inverse relationship of Indonesian rainfall with El Niño is only strong during the dry season (e.g., Ropelewski and Halpert 1987). Despite the persistence of El Niño conditions in the Pacific into the wet season, the contemporaneous relationship of wet season rainfall with El Niño is weak and little predictability based on prior knowledge of the Southern Oscillation is indicated (Nicholls 1981).

Among the other factors that may drive rainfall variability across the Maritime Continent, the effect of local sea surface temperature (SST) anomalies has received considerable attention. Colder than normal local SST is postulated to increase surface pressure and surface divergence, hence reducing rainfall (e.g., Nicholls 1979, Hackert and Hastenrath 1986). But, local SST anomalies, albeit much weaker than those in the central and eastern Pacific, tend to occur in conjunction with El Niño (e.g., Nicholls 1984), thus obfuscating the impact of local and remote forcing. Furthermore, at the onset stages of El Niño (April–September), SST around the–Maritime Continent tends to be colder than normal, and then rapidly warm as El Niño matures at the end of the calendar year (e.g., Rasmusson and Carpenter 1982; Nicholls 1984). These warm SSTs often persist well into the next year, thus exhibiting a biennial character (e.g., Rassmusson et al. 1990). Local air–sea interaction has been hypothesized to explain this seasonality of the SST variations and their biennial tendency (e.g., Nicholls 1979). It is unclear, however, to what extent these much weaker SST anomalies, as compared to those in the central and eastern Pacific, actually force anomalies in local rainfall and circulation. Furthermore, SST variations in the tropical Indian Ocean, which have been postulated to occur independently of El Niño, have also been linked to rainfall variations across Indonesia (e.g., Saji et al. 1999).

This study will build on previous studies of the relationship between Indonesian rainfall and large-scale circulation and SST variations (e.g., Hackert and Hastenrath 1986). Here, monthly rainfall records from 43 stations throughout Indonesia, for the period 1951–97, will be employed to explore relationships between broadscale Indonesian rainfall and circulation and SST anomalies throughout the Indo-Pacific basin. Emphasis will be given to the seasonality of the relationship with El Niño–Southern Oscillation (ENSO) and with local SST. An attempt will be made to synthesize the various hypotheses for the role of remote forcing by ENSO anomalies in the Pacific, of induced biennial variations, and of independent SST variations in the Indian Ocean.

2. Data

Monthly rainfall records from 43 stations throughout Indonesia (Fig. 1) were used in this study (J. McBride, Bureau of Meteorology Research Centre, 2002, personal communication). These stations are a subset of those used by Haylock and McBride (2001), who provide details of their acquisition and quality control. All of the records for these 43 stations are at least 90% complete for the period 1951–97. The focus of this study is on large-scale anomalies; hence, an index of broadscale Indonesian rainfall is formed by simple averaging of all 43 stations (hereafter IndoP). Various other methods for creating an index were tried (e.g., averaging standardized departures from the annual cycle for each station), but little difference in the character of the index was found. Direct averaging of the individual records has the advantage that the index retains physical units (mm month^{-1}). A higher concentration of stations occurs across Java (Fig. 1), which may skew the index to this region. Selectively sampling the stations in this region to the approximate density over the other islands had

little effect on the character of the index and its relation with SST and circulation anomalies. Thus, all of the stations were retained in an attempt to reduce the effects of small-scale noise as much as possible. Prior to creating the index, missing data were replaced with the long-term monthly mean values. Thirty-three stations had less than 5% of the record missing and the other 10 stations had less than 10% missing.

Circulation anomalies are diagnosed with winds from the National Centers for Environmental Prediction–National Center for Atmospheric Research (NCEP–NCAR) reanalyses. Use is also made of the total surface heat flux and its dominant components (latent heat flux and net surface shortwave radiation) in order to diagnose variations in the surface heat budget. Deficiencies in these derived products are acknowledged, but comparison with independent observations suggests that at least the gross behavior of the interannual anomalies is well captured in the reanalyses. SST anomalies are diagnosed using the reconstructed analyses from Smith et al. (1996). All of the above analyses are used for the same 47-yr period as the available rainfall data (1951–97). Anomalies were formed by removal of the trend and the mean seasonal cycle, which was formed by simple averaging of all like months. A 3-month running mean was then applied. Standard seasonal mean data (e.g., December–February) is also employed, which is equivalent to using the central month (e.g., January) of the smoothed data.

3. Annual cycle of rainfall and surface circulation

Indonesia receives substantial rainfall year-round; however, a distinct wet season peaks in January when the large-scale mean rainfall exceeds 250 mm month^{-1} (Fig. 2a). Even during the peak of the dry season (August), upward of 125 mm month^{-1} is received. For convenience, the standard 3-month seasons June–July–August (JJA) and September–October–November (SON) will be referred to as the dry season and December–January–February (DJF) and March–April–May (MAM) as the wet season. More precisely, the dry half of the year extends from May to October, and November is better classified as the early wet season.

The peak of the wet season in January coincides with the northwest monsoon across the Austral–Indonesian region (Fig. 3a). Conversely, the dry season coincides with the southeast monsoon (Fig. 3b). Considering the difference in mean surface winds for DJF and JJA (Fig. 3c) delineates the monsoon region. In this view, the northwest monsoon extends from the western Indian Ocean to the date line. But, the strongest seasonal reversal in surface zonal winds occurs across the Austral–Indonesian region, consistent with the notion that the strongest seasonal rainfall difference occurs here.

Interestingly, the largest absolute interannual variability is seen to occur at the end of the dry season, when the monthly standard deviation exceeds 40 mm month^{-1} and the coefficient of variation (standard deviation divided by the mean) approaches ½ (Fig. 2a). A cursory examination of other monsoon regions (not shown) suggests that the Indonesian region is unique in that the largest absolute variability occurs at the end of

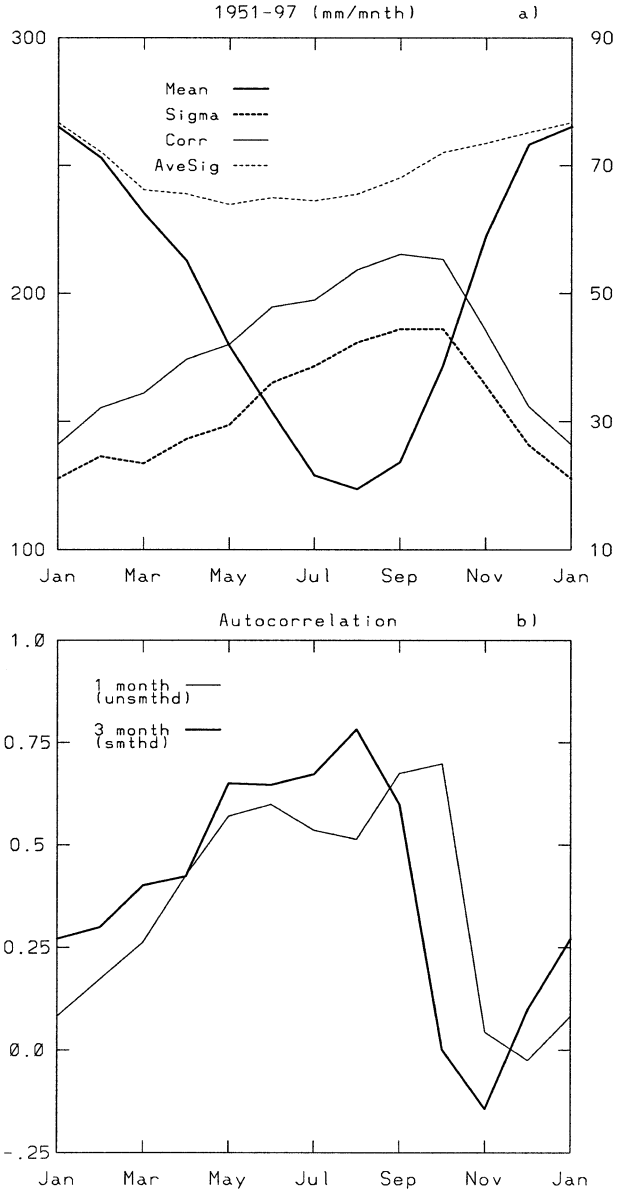

FIG. 2. (a) Seasonal cycle of monthly mean IndoP (heavy solid curve), its std dev (heavy dotted curve), the avg std dev from each of the 43 individual stations (thin dotted curve), and the explained variance (expressed as a correlation coefficient) of the 43 individual stations records by IndoP (thin solid curve). The scale for the mean rainfall is on the left ordinate (mm month^{-1}) and the scale for the std devs (mm month^{-1}) and correlation coefficient ($\times$ 100) is on right ordinate. Data were smoothed with a 3-month running mean prior to computation of means, std devs, and explained variance. (b) Autocorrelation of IndoP at 3-month lead for 3-month mean data (heavy curve) and at 1-month lead for unsmoothed (monthly) data (light curve). Start month is indicated on the abscissa.

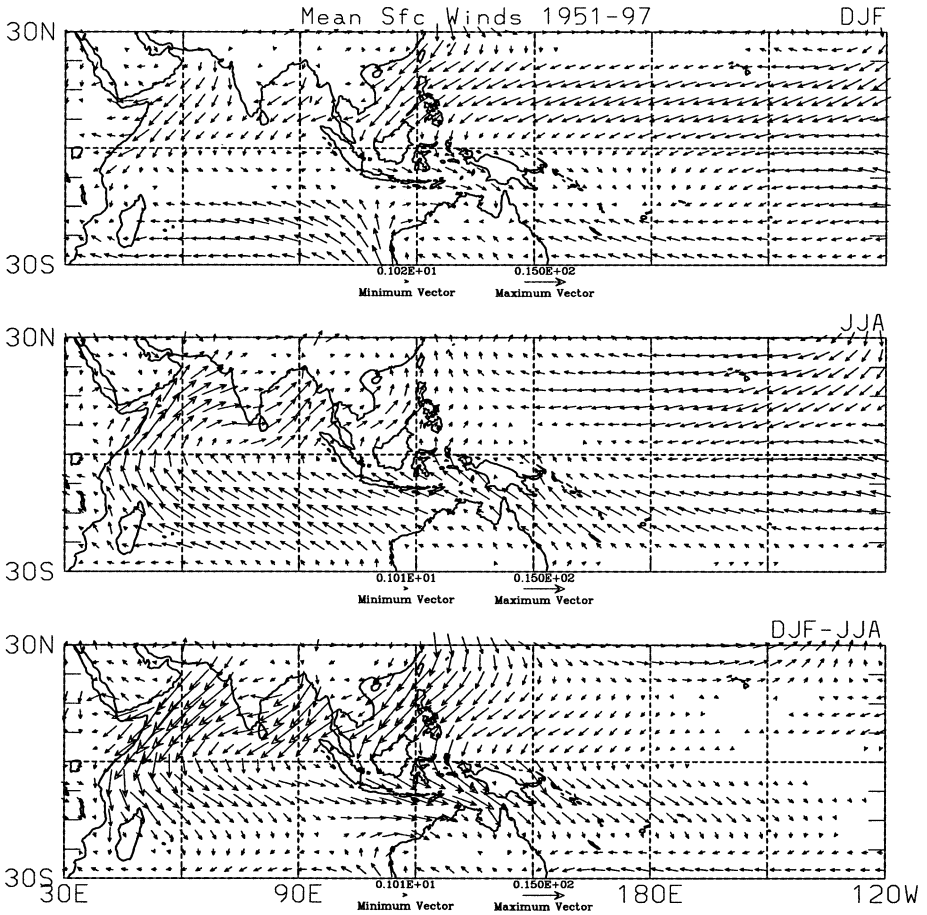

FIG. 3. Mean surface winds for (a) DJF, (b) JJA, and (c) their difference. The averaging period is 1951–97 and the max vector wind difference is 15 m s^{-1}.

the dry season. In other monsoon regions such as India, the Amazon, and Mexico the largest interannual variability tends to coincide with the peak of the wet season. However, the occurrence of largest *relative* variability (i.e., the standard deviation divided by the mean) during the dry season is consistent with the findings of Nicholls and Wong (1990), who show that relative variability of *annual mean* rainfall increases as annual mean rainfall decreases.

Examination of the average standard deviation from each of the 43 individual stations (light dotted curve in Fig. 2a) reveals that variability at individual stations does peak (slightly) during the wet season. Hence, the occurrence of maximum variability of broadscale rainfall (IndoP) during the late dry season implies that the interstation coherence is a maximum then and a minimum during the wet season. Haylock and McBride (2001) reached a similar conclusion by showing that the leading EOF of the Indonesian station rainfall records is broad scale (i.e., one signed across all of Indonesia) during the dry season but is spatially noisy during the wet season. This is substantiated by computation of the explained variance (expressed as a correlation coefficient) at the 43 individual stations by IndoP (thin solid curve in Fig. 2a). IndoP accounts for upward of 30% of the total station variance during the late dry season but dramatically drops to less than 10% at the peak of the wet season. Thus, dry season anomalies are more spatially coherent than their wet season counterparts.

Computation of the autocorrelation of IndoP indicates that dry season anomalies are also dramatically more persistent than their wet season counterparts (Fig. 2b). Based on smoothed data (3-month running mean), anomalies from May to September show strong persistence at 3 months (i.e., the correlation with anomalies 3 months later is better than 0.6), and anomalies from October to February show little persistence (i.e., 3-month lag correlations are less than 0.3). Nicholls (1984) reported similar seasonal variation of persistence of SST anomalies surrounding Indonesia. Examination of the 1-month lag correlation using unsmoothed monthly data suggests that the transition to low persistence occurs abruptly in November, with October anomalies correlating with November anomalies at better than 0.7 but November anomalies being uncorrelated with December anomalies.

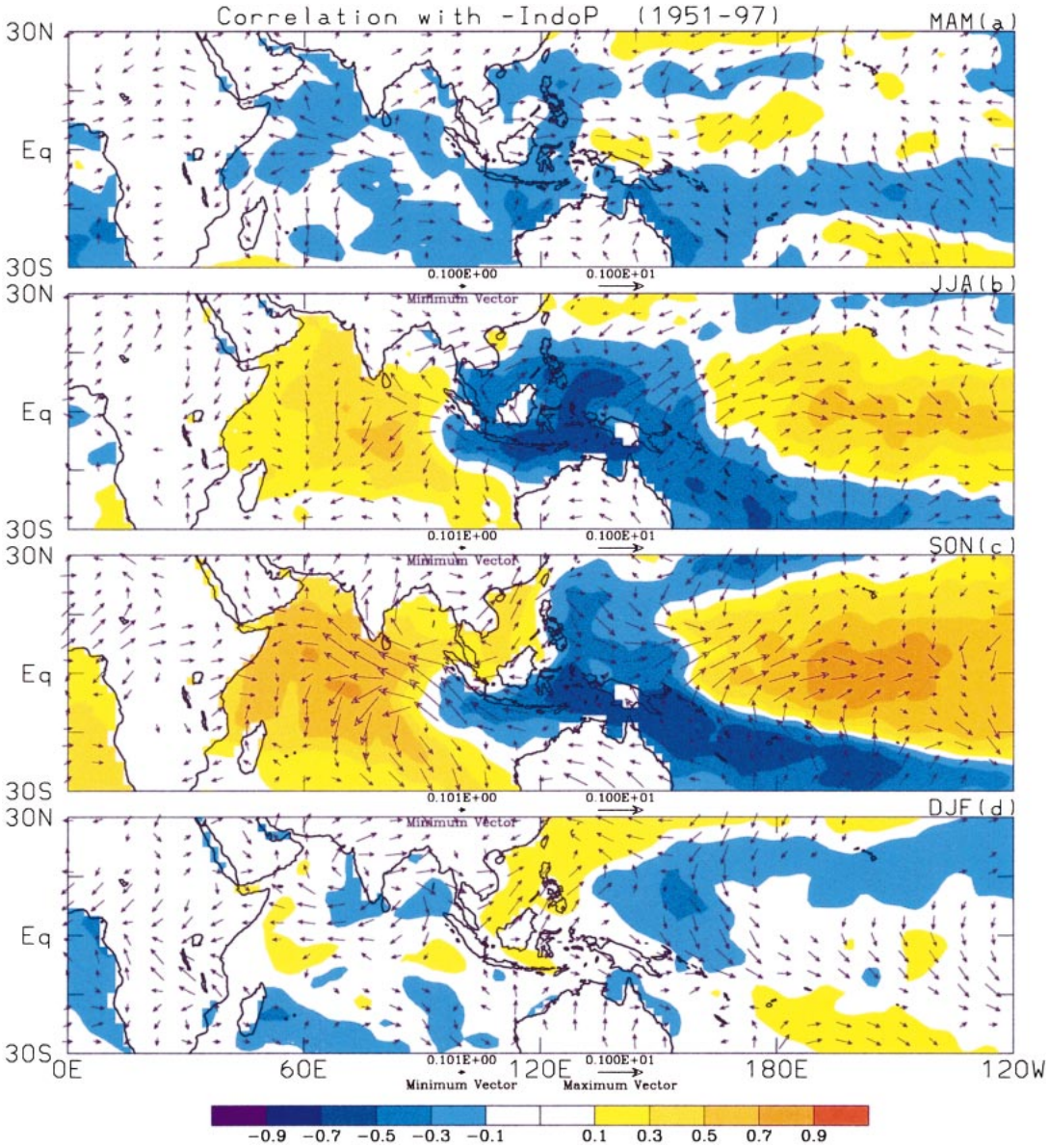

FIG. 4. Simultaneous correlation of −IndoP with SST (shading) and surface winds (max vector is length 1.) for the (a) MAM, (b) JJA, (c) SON, and (d) DJF seasons. A correlation of approximately 0.24 is significantly different than zero at the 95% confidence level, assuming 46 degrees of freedom (i.e., assuming each year is independent).

4. Seasonal relationship with SST, circulation, and ENSO

Seasonal relationships between Indonesian rainfall, SST, and circulation throughout the Indo-Pacific basin are explored by correlating seasonal mean IndoP with gridpoint values of SST and surface winds. Because of the well-known correspondence of drought conditions with warm phases of ENSO (e.g., Kiladis and Diaz 1989), the sign of IndoP is flipped prior to computing the correlation so that relationships with Indonesian drought are depicted. Below-normal IndoP during the dry season (JJA and SON; Figs. 4b,c) tends to occur in conjunction with warm SSTs in the central Pacific, locally cold SSTs surrounding the Maritime Continent, and warm SSTs in the western Indian Ocean. In marked contrast, IndoP during the wet half of the year (DJF and MAM) tends to be unrelated to SST (Figs. 4a,d).

Also shown in Fig. 4 is the correlation of IndoP with surface wind at each grid point. Drought conditions during the dry season (Figs. 4b,c) are accompanied by surface southeasterlies across and to the west of Indonesia, which diverge from the region of locally cold SST and suppressed rainfall. Their structure is consistent with the steady response to localized anomalous cooling dis-

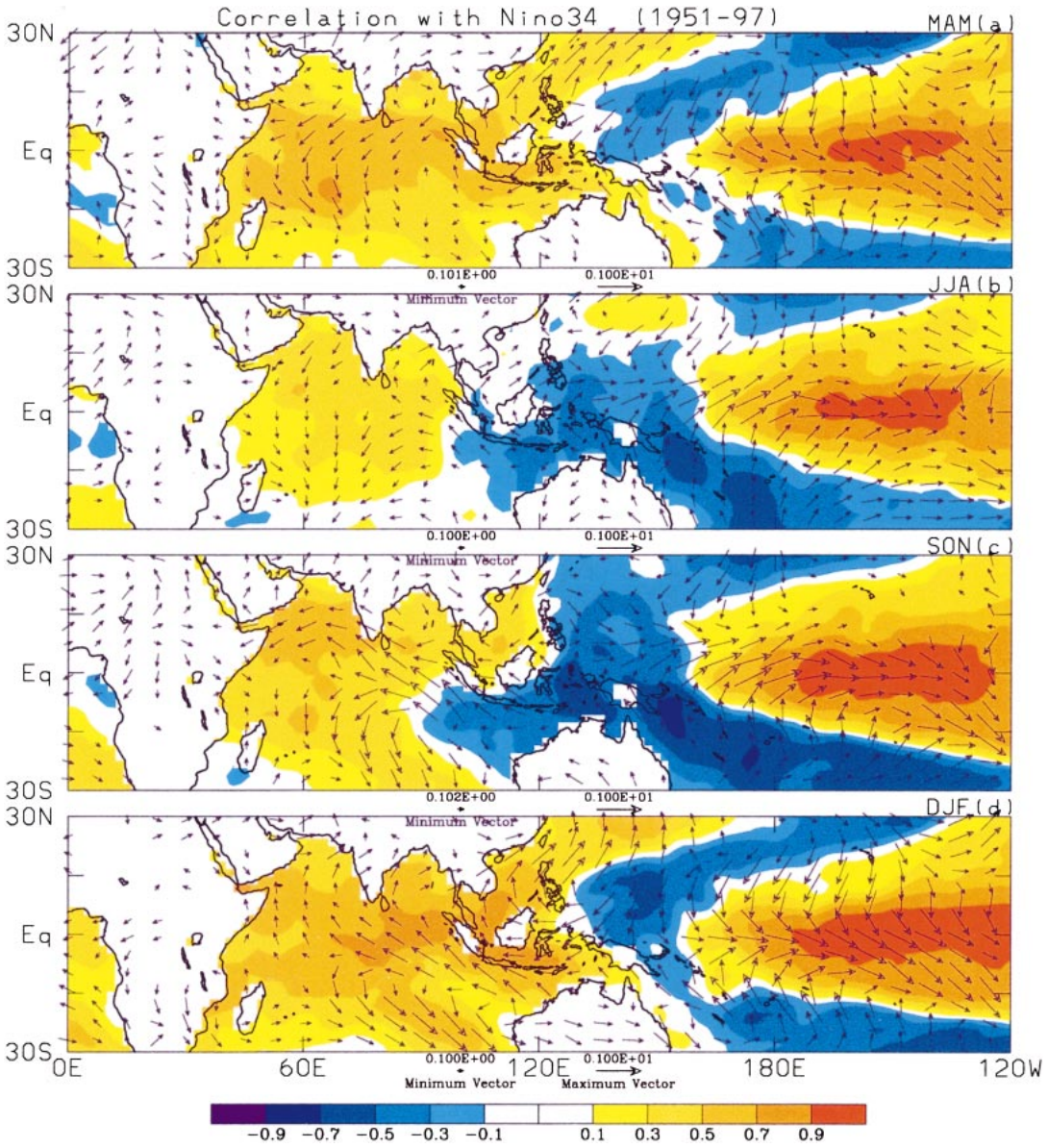

FIG. 5. Seasonal correlation of Niño-3.4 with SST and surface winds for (a) MAM, (b) JJA, (c) SON, and (d) DJF. Plotting convention is same as in Fig. 4.

placed south of the equator (e.g., Gill 1980). The divergent southeasterlies extend well south and west of Indonesia and coincide with the broad cold SST anomaly. Implied is that dry season rainfall variations across Indonesia are indicative of rainfall variations across a broader domain, roughly extending from 15°S to the equator and 100° to 135°E. During the wet season (Figs. 4a,d), when significant correlations with SST are absent, little structure in the surface wind field is evident.

The SST anomalies associated with reduced rainfall in the dry season are indicative of the warm phase of ENSO (El Niño), which is emphasized by considering the seasonal correlation of Niño-3.4 (SST averaged 5°S–5°N, 170°–120°W) with SST (Fig. 5). Niño-3.4 is used as the index of ENSO because SST variations in this region are associated with the convective anomalies that accompany the Southern Oscillation (e.g., Deser and Wallace 1990), hence, with rainfall variations in the Indonesian region (e.g., Nicholls 1981). The close correspondence of Figs. 4b,c with Figs. 5b,c confirm the strong connection between dry season drought and El Niño. The warm anomalies in the western Indian Ocean and the cold anomalies in the eastern Indian Ocean/far western Pacific, while not receiving as much attention as their warm counterpart in the central and eastern Pacific, are typical conditions of El Niño during the JJA and SON seasons (e.g., Rasmusson and Carpenter 1982; Nicholls 1984).

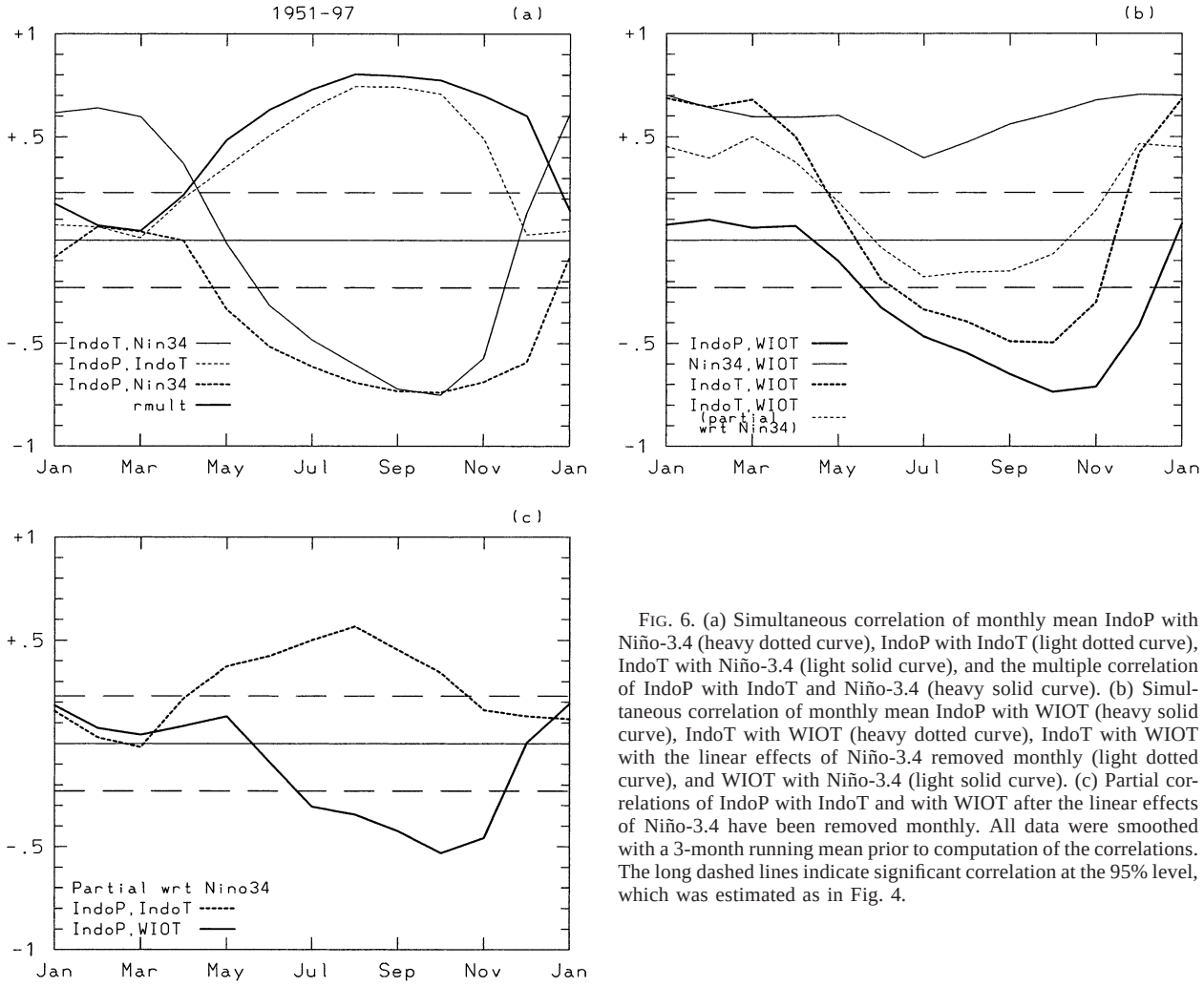

FIG. 6. (a) Simultaneous correlation of monthly mean IndoP with Niño-3.4 (heavy dotted curve), IndoP with IndoT (light dotted curve), IndoT with Niño-3.4 (light solid curve), and the multiple correlation of IndoP with IndoT and Niño-3.4 (heavy solid curve). (b) Simultaneous correlation of monthly mean IndoP with WIOT (heavy solid curve), IndoT with WIOT (heavy dotted curve), IndoT with WIOT with the linear effects of Niño-3.4 removed monthly (light dotted curve), and WIOT with Niño-3.4 (light solid curve). (c) Partial correlations of IndoP with IndoT and with WIOT after the linear effects of Niño-3.4 have been removed monthly. All data were smoothed with a 3-month running mean prior to computation of the correlations. The long dashed lines indicate significant correlation at the 95% level, which was estimated as in Fig. 4.

On the other hand, the contrast of El Niño conditions during MAM (Fig. 5a) and DJF (Fig. 5d) with the lack of correlation of SST with rainfall in these seasons (Figs. 4a,d) is remarkable. This lack of resemblance, as will be elucidated below, stems from the contrasting behavior of SSTs in the eastern Indian Ocean between the dry and wet seasons. During El Niño, the entire Indian Ocean tends to be warm in DJF and MAM (Figs. 5d,a). This basin-scale warming typically lags the peak warming in the east Pacific by about 3–4 months (e.g., Klein et al. 1999). But, the stratification of the correlations by season emphasizes its occurrence is tightly tied to the seasonal cycle. In JJA and SON during El Niño the eastern Indian Ocean tends to be cold (e.g., Rasmusson and Carpenter 1982; Nicholls 1984), giving rise to a negative zonal SST gradient reminiscent of the ''dipole'' described by Webster et al. (1999) and Saji et al. (1999). Note also the strong similarity of the correlations based on Niño-3.4 during JJA and SON with those based on −IndoP (Figs. 4b,c). Hence, both the negative zonal SST gradient in the Indian Ocean and the positive zonal SST gradient in the Pacific promote reduced rainfall in JJA and SON. The reduction of these anomalous gradients in MAM and DJF during El Niño (Figs. 5a,d) appears to be at the root of the lack of correlation of rainfall with SST in these seasons (Figs. 4a,d).

These seasonally varying relationships between Indonesian rainfall and SST are explored in more detail in Fig. 6a. Correlations by month are shown for IndoP (*without the sign flipped*) with Niño-3.4 and with SST surrounding Indonesia (0°–10°S, 95°–135°E, hereafter IndoT). IndoT was chosen because it is the region with strongest correlation with IndoP (Figs. 4b,c) and Niño-3.4 (see Figs. 5b,c). Figure 6a demonstrates that significant positive correlation of IndoT with IndoP is confined to the dry half of the year (May–October), but the negative correlation of IndoP with Niño-3.4, while peaking in the dry season, extends into the early wet season (December). Implications for predictability of early wet season rainfall, based on the status of ENSO at the end of the dry season (e.g., Nicholls 1981) are discussed in section 7. It is noteworthy that the peak negative cor-

relation with Niño-3.4 and peak positive correlation with IndoT occurs when IndoT and Niño-3.4 are strongly anticorrelated (thin solid curve in Fig. 6a). Furthermore, the lack of negative correlation of IndoP and Niño-3.4 during January–April occurs when Niño-3.4 and IndoT are positively correlated. Again, this emphasizes that IndoP is sensitive not only to local SST variations but to large-scale SST gradients as well. The multiple correlation of IndoP with Niño-3.4 and IndoT[2] (heavy curve in Fig. 6a) indicates that very little independent information comes from each of the SST time series, except in December, when correlation of IndoP with IndoT goes to zero but remains significantly negative with Niño-3.4.

The out-of-phase relationship of IndoP and west Indian Ocean SST during the dry season, as suggested in Figs. 4b,c, is emphasized by correlating monthly IndoP (*without the sign flipped*) with SSTs averaged across the western Indian Ocean (5°S–10°N, 45°–75°E, hereafter WIOT). The heavy solid curve in Fig. 6b indicates that significant negative correlation between IndoP and WIOT is confined to June–December. At these times, SSTs at opposite sides of the Indian Ocean also tend to be anticorrelated (heavy dotted curve in Fig. 6b). From January to May, when SST anomalies across the Indian Ocean tend to have the same sign, little correlation between IndoP and WIOT occurs. Thus, drought across Indonesia during the dry season tends to occur in the presence of an anomalously negative zonal gradient in SST across the Indian Ocean (Fig. 6b) together with an anomalously positive zonal gradient across the Pacific (Fig. 6a).

These seasonal correlations (Figs. 4 and 5) emphasize that the anomalous zonal SST gradient in the Indian Ocean and the concomitant IndoP anomalies are typical expressions of the ENSO cycle during the dry season (June–November). SST in the western Indian Ocean is positively correlated with Niño-3.4 throughout the year (thin curve in Fig. 6b), while the correlation with Niño-3.4 at the eastern side (i.e., with IndoT) changes sign from negative during the dry season to positive during the wet season (thin curve in Fig. 6a). Furthermore, the partial correlation of IndoT and WIOT (thin dotted curve in Fig. 6b) reveals that the negative correlation of SSTs across the Indian Ocean Basin during the dry season disappears once the linear relationship with Niño-3.4 is removed.[3] Note that this partial correlation was computed by month, so that the monthly varying (but simultaneous) relationships with Niño-3.4 depicted in Figs. 6a,b were removed. That is, the ENSO signal removed in the dry season is characterized by out-of-phase behavior of SST across the Indian Ocean, while that removed during the wet season is in-phase behavior. Interestingly, it is the *in-phase* fluctuation (i.e., the signal normally associated with ENSO) of SST across the Indian Ocean during the *wet season* that appears to have a large degree of independence from ENSO.

Despite the fact the SSTs across the Indian Ocean tend not to be anticorrelated in the absence of ENSO and thus not as conducive for promoting anomalous IndoP, it is still interesting to explore what sort of relation the SST variations independent of ENSO might have with IndoP. Recall that Niño-3.4 (Fig. 6a) accounts for only 50% of the variance of IndoP during the dry season. The partial correlations of IndoP with IndoT and IndoP with WIOT (Fig. 6c) indicate that upward of 25% of the dry season rainfall variance that is unaccounted for by ENSO can be explained by independent variations in IndoT and WIOT. The sense of these partial correlations is similar to the total correlations (Figs. 6a,b), with reduced dry season rainfall associated with negative IndoT anomalies and positive WIOT anomalies. Even though SST anomalies at opposite sides of the Indian Ocean tend not to be anticorrelated in the absence of ENSO, IndoP variations are still associated with an anomalous zonal SST gradient in the Indian Ocean. A plausible interpretation of these partial correlations is that IndoP responds to the anomalous zonal SST gradient, regardless of whether an SST anomaly only occurs on one side of the basin. However, the magnitude of these partial correlations is put into perspective by taking into account that roughly 50% of the rainfall variance is unaccounted by Niño-3.4. Hence, only about 10%–15% of the *total* rainfall variance is accounted for by SST variations in these regions that are independent of ENSO. Further work is required to determine whether different processes govern these SST variations than those associated with ENSO and whether they can provide additional predictability of IndoP.

5. Evolution of dry season anomalies

The picture that emerges from the analysis to this point is that IndoP variations are predominantly accounted for by ENSO in those seasons during which the local SST anomalies associated with ENSO act in unison with those in the Pacific and western Indian Oceans to weaken the Walker circulation. In the seasons when the local SST anomalies associated with ENSO have the same sign as those in the central and eastern Pacific and western Indian Oceans, little relationship of IndoP with ENSO is evident. Further insight into these seasonally varying relationships is gained by examination of the evolution of anomalies from the dry season into the wet season. Figure 7 displays various lag correlations with respect to −IndoP (i.e., the time series of IndoP with

[2] The magnitude of the multiple correlation of IndoP with IndoT and Niño-3.4 is given by $|r_{3.21}| = [(r_{31}^2 + r_{32}^2 - 2r_{31}r_{32}r_{12})/(1 - r_{12}^2)]^{1/2}$, where r_{31} is the correlation of IndoP with IndoT, r_{32} is the correlation of IndoP with Niño-3.4, and r_{12} is the correlation of Niño-3.4 with IndoT.

[3] The partial correlation of IndoT with WIOT, where the linear relationship with Niño-3.4 is removed from both time series, is given by $r_{13.2} = (r_{13} - r_{12}r_{23})/(\sqrt{1 - r_{12}^2}\sqrt{1 - r_{23}^2})$, where r_{13} is the correlation of IndoT with WIOT, r_{12} is the correlation of IndoT with Niño-3.4, and r_{23} is the correlation of WIOT with Niño-3.4.

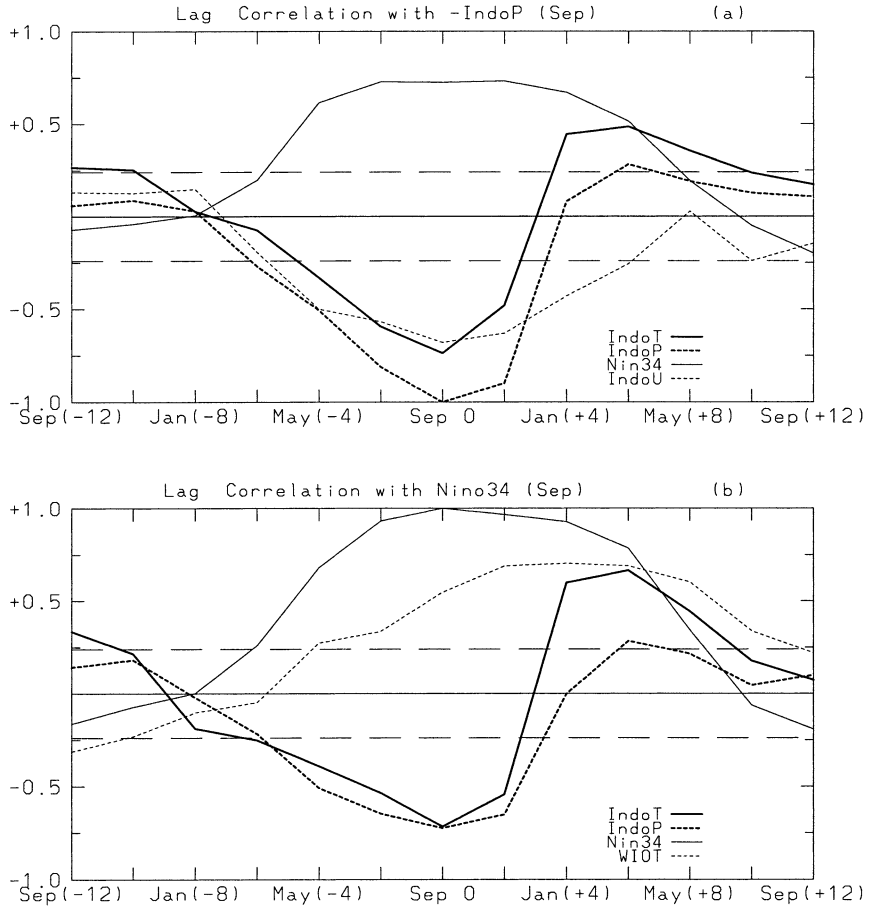

FIG. 7. (a) Lagged correlation of Sep mean −IndoP (i.e., the time series of IndoP in Sep with the sign flipped) with monthly mean IndoT (heavy solid curve), IndoP (heavy dotted curve), Niño-3.4 (light solid curve), and IndoU (light dotted curve). Correlations are displayed for −IndoP leading by 12 months (Sep − 12) to −IndoP lagging by 12 months (Sep + 12). (b) As in (a) except correlations are with respect to Niño-3.4 in Sep and the light dotted curve is now for WIOT. All data were subjected to a 3-month running mean prior to computation of the correlations. Significant correlation is estimated as in Fig. 4.

the sign flipped) and with respect to Niño-3.4 in September. The evolution depicted by the correlations with respect to −IndoP (Fig. 7a) is nearly identical to that with respect to Niño-3.4 (Fig. 7b). The evolution seen in Fig. 7a can be taken to be typical of ENSO: dry conditions in September are preceded by warm SSTs in the central and eastern Pacific (as early as the preceding April) and in the western Indian Ocean (as early as the preceding July) and by locally cold SSTs beneath divergent surface easterlies throughout the Maritime Continent (as early as the preceding May). The warm anomaly in the central and eastern Pacific is maintained through the following April, with the peak warming in the western Indian Ocean lagging that in the east Pacific by about 3–5 months (e.g., Klein et al. 1999). Dry conditions across Indonesia from June to November thus occur in conjunction with an anomalously negative zonal SST gradient in the Indian Ocean and a positive gradient in the Pacific. This negative zonal gradient in the Indian Ocean rapidly diminishes in November, when SSTs in the Indonesian/eastern Indian Ocean region warm. Thus, explanation of the loss of correlation of IndoP with local and remote SST in the wet season is tantamount to understanding why local SSTs rapidly warm up during El Niño once the wet season commences.

A critical component of the seasonally phase-locked behavior of El Niño is the easterly to southeasterly surface wind anomalies, which accompany dry–cold conditions in Indonesia during SON (e.g., Figs. 4c and 5c), but that continue into the start of the wet season (Fig. 5d), even though the local SSTs have rapidly warmed. The surface zonal wind anomaly averaged over the same box as IndoT (hereafter IndoU), in fact, tracks the evolution of Niño-3.4 much better (but with opposite sign; Fig. 7a). The surface zonal wind anomaly across Indonesia is thus better viewed as the response to the Indo-Pacific basin-scale SST anomalies than it is to just local

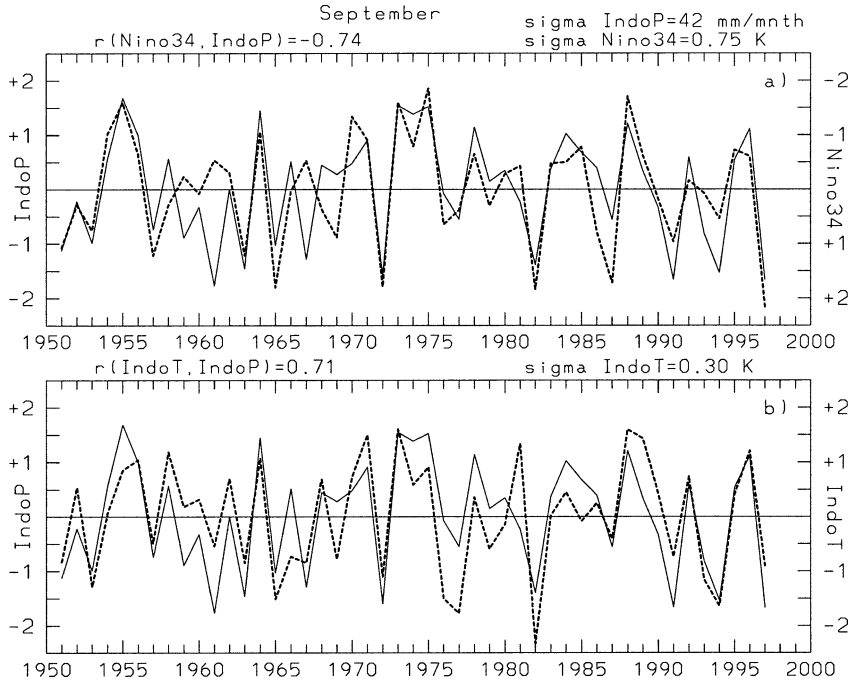

FIG. 8. Time series of (a) IndoP (solid) and Niño-3.4 (dashed; note scale is flipped for Niño-3.4) and (b) IndoP (solid) and IndoT (dashed) for Sep 1951–97. Ordinates are labeled in std dev, with the std dev for each field indicated above the plot.

SST and rainfall anomalies. This nonlocal view is counter to that often adopted to explain biennial variations in this region (e.g., Nicholls 1979; Clarke et al. 1998). However, it does not suffer from the problem of trying to explain the observed lag of 3–4 months between local SST (or rainfall) and surface zonal wind. It also is able to account for the local zonal wind anomaly (IndoU) being out of phase with the local rainfall (IndoP) and SST (IndoT) anomalies from December to April (Fig. 7a). Below, it will be demonstrated that maintenance of these southeasterlies into the wet season helps explain the continued warming of IndoT, hence, the subsequent loss of negative correlation with Niño-3.4.

The physical mechanism that causes IndoT to cool during the developing stages of El Niño (June–September) and then to rapidly warm as El Niño matures (October–February) is elucidated using composites based on dry and wet conditions across Indonesia during September, which is when the correlation of IndoP and IndoT with Niño-3.4 is most negative. Dry and wet years are defined when IndoP exceeds minus and plus one standard deviation (Fig. 8). These years are listed in Table 1. A similar evolution is obtained if the years are identified based on excursions of Niño-3.4 (recall that IndoP and Niño-3.4 SST are negatively correlated at about 0.7 during September). However, there are some notable discrepancies (e.g., 1961 and 1967; see also Saji et al. 1999), when strong anomalies in IndoT and IndoP are not accompanied by significant opposite-signed anomalies in Niño-3.4. However, consistent with the strong negative correlation of Niño-3.4 and IndoP (~ -0.7), this is the exception rather than the rule.

TABLE 1. Wet and dry years for the period 1951–96, based on occurrence of one std dev anomalies of IndoP (subjected to a 3-month running mean) during Sep.

Wet	Dry
1955, 1956, 1964, 1973, 1974, 1975, 1978, 1984, 1988, 1996	1951, 1953, 1961, 1963, 1965, 1967, 1972, 1982, 1991, 1994

Anomalies during wet years are essentially opposite sign to those during dry years, so composite anomalies are developed as (Dry – Wet)/2. Composites of rainfall, SST, and surface fluxes across the Indonesian region are formed in order to elucidate the role of local air–sea interaction for producing the observed evolution.

During September, a rainfall deficit of about 60 mm month^{-1} (Fig. 9a) is accompanied by a negative IndoT anomaly of about 0.25 K and a positive Niño-3.4 anomaly of 1 K. The evolution of these anomalies is entirely consistent with the lag correlations shown in Fig. 7a. Dry and cold conditions across Indonesia during September rapidly decay and change sign at the start of the year, while Niño-3.4 does not decay until some 4 or 5 months later.

Examination of the net surface heat flux averaged for the same box as IndoT (heavy dotted curve in Fig. 9b) reveals that it leads IndoT by about 2–3 months, which is consistent with the notion that the surface heat flux variation is driving the change in IndoT. The magnitude

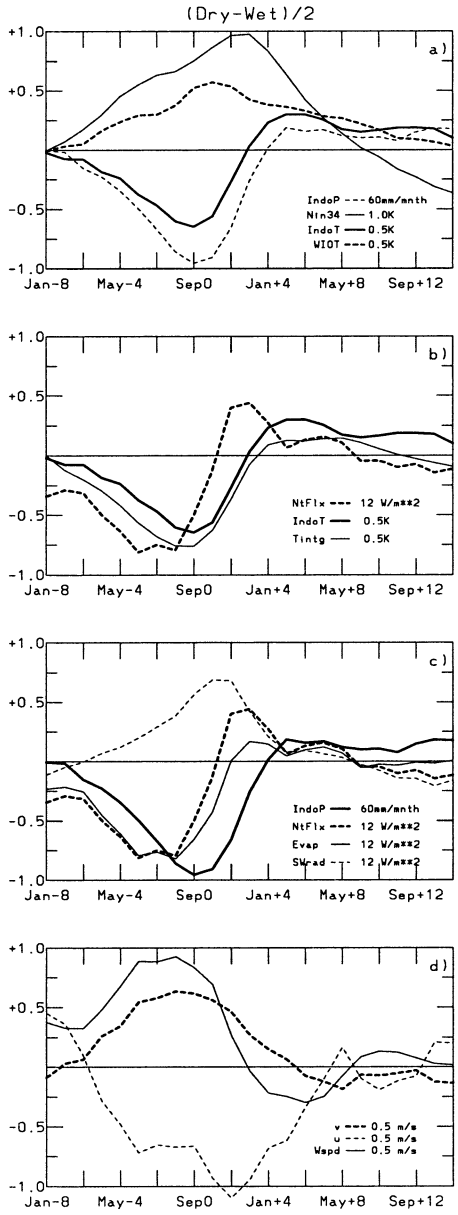

FIG. 9. Dry minus wet composites (divided by 2) based on occurrences of one std dev anomalies of IndoP in Sep (years indicated in Table 1). Shown are monthly composite time series of (a) Niño-3.4 (light solid curve), IndoT (heavy solid curve), WIOT (heavy dotted curve), and IndoP (heavy dotted curve); (b) IndoT (heavy solid curve), total surface heat (heavy dotted curve), and the predicted SST by Eq. (1) (light dotted curve); (c) IndoP (heavy solid curve), net surface heat flux (heavy dotted curve), latent heat flux (light solid curve), and surface shortwave radiation (light dotted curve); and (d) wind speed (light solid curve), surface zonal wind (light dotted curve), and surface meridional wind (heavy dotted curve). The abscissa is labeled in months relative to Sep and runs from −8 to +13 months. The anomalies of net heat flux, shortwave radiation, latent heat flux, wind speed, and surface winds were averaged over the same domain as IndoT (i.e., 0°–10°S, 100°–135°E). The scale of the ordinate for each variable is indicated in the lower right of each panel. Composites were smoothed with a 3-month running mean.

of the surface heat flux variation is sufficient to account for the observed temperature variation as demonstrated by the integration of a simple one-dimensional model of the mixed-layer temperature driven by the observed surface heat flux:

$$\frac{\partial T}{\partial t} = \frac{F}{h\rho C_p} - \lambda T. \tag{1}$$

Here, T is the mixed-layer temperature anomaly, F is the composite net surface heat flux anomaly, h is the mixed-layer depth, ρ is the density of water, C_p is the specific heat, and $-\lambda T$ represents upper-ocean processes that dissipate heat from the mixed layer (e.g., penetrative short-wave radiation, advective processes, vertical mixing). Equation (1) is integrated from the January preceding the peak anomalies in September. The initial temperature anomaly is set to zero. The resulting temperature anomaly, using reasonable values of $h = 30$ m (e.g., Levitus 1982) and $\lambda = 2$ month^{-1}, is shown as the thin solid line in Fig. 9b. Similar amplitude and phasing is obtained, for instance, with $h = 40$ m and $\lambda = 3$ month^{-1}. The phasing of the initial cooling and phasing and magnitude of the subsequent warming are well captured, but the initial cooling is somewhat overestimated. Deficiencies in the model (e.g., neglect of ocean dynamics) and the heat flux are probable. But, the overall agreement suggests that the surface heat flux variation is a major contributor to the sea surface temperature variation associated with ENSO in the eastern Indian Ocean/Indonesian region (see also Klein et al. 1999).

Examination of the dominant terms in the surface heat budget (latent heat flux and short-wave radiation) shows that the development of cold IndoT during the dry season occurs initially in conjunction with increased latent heat flux (magnitude 10 W m^{-2}; Fig. 9c). By August, the latent heat flux anomaly begins to weaken, while a positive surface shortwave radiation anomaly develops in association with suppressed rainfall. Subsequently, IndoT warms dramatically (cf. Hackert and Hastenrath 1986). Note that the shortwave radiation anomaly tracks the evolution of the rainfall anomaly. That is, increased surface shortwave radiation occurs in conjunction with decreased rainfall, which is presumably associated with decreased cloud cover. This close correspondence suggests that at least the qualitative evolution of the shortwave radiation anomaly is captured in the reanalysis.[4] By November, the latent heat flux anomaly has become negative (reduced evaporation) and now acts in conjunction with the shortwave radiation anomaly to warm IndoT. By the start of the year weakly positive anomalous SSTs appear.

The evolution of the latent heat flux (i.e., its change

[4] The slight lag of the shortwave radiation anomaly with respect to IndoP may stem from the nonuniform spacing of the stations used in creating IndoP (Fig. 1).

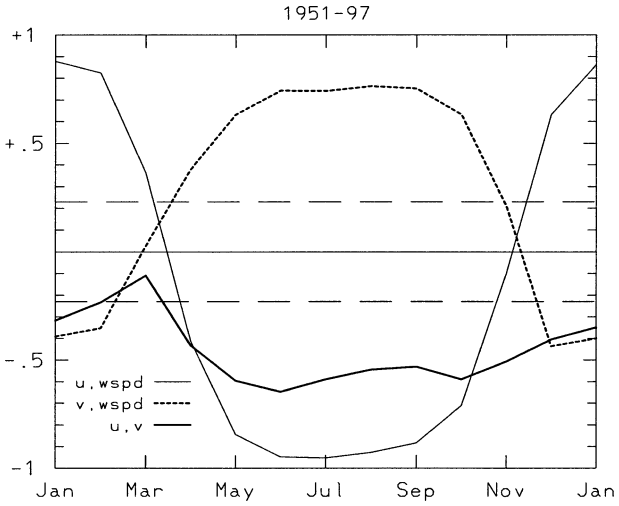

FIG. 10. Simultaneous correlation of monthly mean anomalies of surface zonal wind and wind speed (light solid curve), surface meridional wind and wind speed (heavy dotted curve), and surface zonal and meridional winds (heavy solid curve). All fields were averaged over the same domain as IndoT (i.e., 0°–10°S, 100°–135°E) and subjected to a 3-month running mean prior to computing correlation.

in sign from September to December) is well explained by the evolution of surface wind speed (Fig. 9d). Importantly, however, the wind speed anomaly changes sign in November while the zonal and meridional wind components keep the same sign until March. Implied then is that a southeasterly anomaly in the dry season (June–November) increases the wind speed while a southeasterly anomaly in the wet season decreases the wind speed. This change in the sense of how anomalies in the zonal and meridional winds produce a change in wind speed anomaly reflects the seasonal change in basic-state winds associated with the Australian summer monsoon (e.g., Fig. 3).

This seasonally varying relationship between anomalous wind direction and wind speed in the Indonesian region is summarized in Fig. 10. During the dry season anomalous easterlies and southerlies are positively correlated with enhanced wind speed. The opposite is true during the wet season. The transition between the two regimes is rather abrupt, emphasizing the sharpness of the monsoon in this region (e.g., Hendon and Liebmann 1990). Furthermore, throughout the year zonal and meridional wind anomalies in the Indonesian region are negatively correlated, thus implying that anomalies in one component tend to act in unison with anomalies in the other to affect the wind speed. The negative correlation between the two individual wind components throughout the year is consistent with the notion that surface wind anomalies in this region are driven, at least partially, by anomalous, off-equatorial, diabatic heating associated with large-scale rainfall anomalies. As anticipated by the steady response to heating displaced south of the equator (Gill 1980), northwesterlies converge into imposed heating and southeasterlies diverge out of imposed cooling.

The composite analysis presented in Fig. 9 suggests that a positive feedback between wind speed and IndoT occurs during the dry season and a negative feedback develops during the wet season (e.g., Nicholls 1979). During the dry season, decreased rainfall and surface southeasterlies accompany cold IndoT. The southeasterlies act to increase the wind speed, thereby increasing evaporative cooling and turbulent mixing. IndoT further cools, which decreases rainfall. During the wet season, the same anomalous southeasterlies would act to decrease the wind speed, thus warming IndoT, increasing rainfall, hence diminishing the southeasterlies. A critical component, then, of understanding the evolution of rainfall and SST anomalies in the Indonesian region is to explain why the local wind (circulation) anomalies tend to persist well into the wet season while the local SST and rainfall anomalies change sign at the onset of the wet season. This behavior needs to be understood with the realization that local SST anomalies do not occur in isolation and that the local circulation anomalies are affected by SST anomalies across the entire Indo-Pacific basin.

The role of anomalous SST throughout the Tropics for controlling the surface wind anomalies across Indonesia is illuminated by diagnosis of variations of the Walker circulation. Here, variations in the Walker circulation are diagnosed with the ''zonal mass flux'' developed by Newell et al. (1974):

$$M(p) = \frac{r_e \Delta\phi}{g} \int_{p_s}^{p} \langle u' \rangle \, dp,$$

where r_e is the radius of the earth, $\Delta\phi = 10°$ is the latitude increment, and $\langle u' \rangle$ is the eddy zonal wind averaged over the latitude band 5°S–5°N. While not a direct measure of the equatorial overturning circulation, M has the benefits of being readily computed, a scalar field and easily contoured. For sufficient latitudinal averages about the equator such that the meridional divergence is weak, M measures the strength of the Walker circulation. Comparison with the actual divergent circulation in the equatorial plane indicates that M provides a good approximation (Bergman and Hendon 2000).

Figure 11 displays the dry–wet composites of M, along with standardized SST anomalies averaged 5°N–5°S, for 3 months prior (June − 3) to 3 months after (Dec + 3) dry conditions in September. Dry conditions across Indonesia during September coincide with an weakened Walker circulation, with the enhanced rising collocated with warm SST anomalies in both the western Indian and central Pacific Oceans and the anomalous downward branch collocated with cold SSTs centered on Indonesia. From this perspective, anomalous easterlies across the eastern Indian Ocean and Indonesia, which were argued to feed back positively during the dry season to further decrease the local SST by increas-

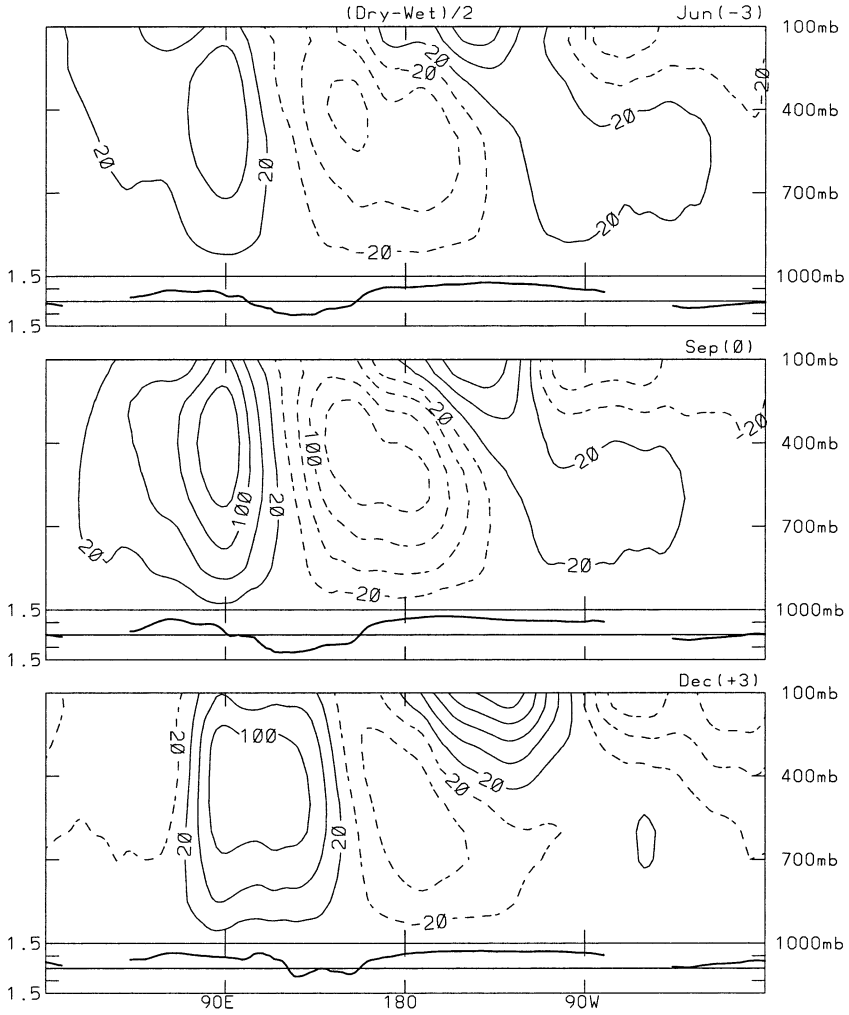

FIG. 11. Dry–wet composite anomalies (divided by 2) of monthly mean *M*, the zonal mass flux (defined in text), and equatorially averaged SST (5°N–5°S) based on occurrences of one std dev anomalies of IndoP for Sep (years indicated in Table 1). Shown are anomalies for (a) the preceding Jun (−3 months), (b) the concurrent Sep, and (c) the following Dec (+3 months). The *M* anomalies (smoothed with a 3-month running mean) are contoured (contour interval 4 × 10^9 kg s^{-1}; first contour at ±2 × 10^9 kg s^{-1}). The direction of implied motion in the equatorial zonal-height plane is clockwise around positive centers and counterclockwise around negative centers. The SST composite was formed from standardized anomalies at each lon, after initially smoothing with a 3-month running mean. The units on the left ordinate are std devs.

ing the wind speed and latent heat flux, stem from an anomalous Walker circulation driven by Indo-Pacific basin-scale changes in SST. As such, the continuation of easterly surface anomalies at Indonesian longitudes during December, even when the local SST and rainfall anomalies have decayed to near zero, are best viewed as being driven by the anomalous Walker circulation, which responds to SST anomalies throughout the Tropics.

6. Biennial variations

The fact that anomalous surface southeasterlies tend to continue across the Indonesian region well into the wet season, even after the local SST anomaly has gone to zero or changed sign (e.g., Fig. 7a), has important implications for generation of biennial variations of SST and rainfall. Biennial variations of SST in the Indonesian region are postulated to come about because ENSO-related SST anomalies in the central and eastern Pacific typically persist into the early calendar year before changing sign. Thus, they can provide the necessary forcing of the local winds across Indonesia that can drive the local SST from one sign, prior to onset of the wet season in October–November, to the opposite sign by the end of the wet season in March–April. The positive feedback between local SST and surface winds during

the subsequent dry season (May–October) can then help to maintain the SST anomaly up until the onset of the following year's wet season (see also Clarke et al. 1998). This interpretation is different than Meehl (1993), who proposes that biennial variations arise because convection selectively interacts with SST anomalies just during the wet season. Here, it is argued that there is positive feedback during the dry season and negative feedback during the wet season, but remote forcing from ENSO is what is able to carry an anomaly through the wet season and into the next dry season.

The frequency spectrum of IndoT, in fact, does exhibit a significant biennial peak (Fig. 12a). On the other hand, east Pacific SSTs exhibit only a hint of elevated power at biennial periods, with the main peak associated with ENSO occurring at 4–6-yr periods (Fig. 12b). However, peak coherence of the two time series occurs in the biennial band (1.5–2.5 yr; Fig. 12c). At these periods, IndoT leads Niño-3.4 by about 3–4 months, consistent with the composites shown in Fig. 7. Thus, the observed biennial tendency in SST and rainfall in the Indonesian region during the ENSO cycle (Fig. 9; e.g., Kiladis and Diaz 1989; Rasmusson et al. 1990) can be viewed as the local expression of the ENSO cycle, even though ENSO itself does not necessarily exhibit a strong biennial tendency.

7. Discussion and conclusions

Indonesian rainfall is highly coherent with local and remote SSTs during the dry half of the year (May–October) but uncorrelated with SST during the peak of the wet season (January–March). Drought conditions during the dry season typically occur in conjunction with the development of El Niño in the Pacific, when anomalously cold SSTs typically surround Indonesia while warm anomalies develop in the eastern Pacific and western Indian Oceans (cf. Rasmusson and Carpenter 1982). Conversely, enhanced Indonesian rainfall during the dry season typically occurs during the development of La Niña, with SST anomalies opposite to those of El Niño. The accompanying circulation anomalies during the dry season are consistent with these SST anomalies: diminished rainfall is accompanied locally by anomalous surface southeasterlies and the large-scale sinking motion, indicative of a weakened Walker circulation.

Broadscale Indonesian rainfall anomalies also tend to persist in the dry season but not in the wet season. The lack of persistence and correlation with SST in the wet season results because, during the development of ENSO, the local SST anomalies surrounding Indonesia abruptly change sign during the transition from the dry to the wet season (cf. Nicholls 1984). Hence, during the dry season the local impact of anomalous SSTs on rainfall and the Walker circulation tends to compound that due to the remote SSTs (cf. Rowell 2001). During the wet season, the local impact of the SSTs tends to oppose or cancel that produced by the remote SSTs.

Despite the rapid loss of correlation with SST once the wet season commences, useful predictability of late dry season rainfall, based on persistence of ENSO through the dry season, is implied (see also Nicholls 1981). Lag correlations with September IndoP (Fig. 7a) indicate that a strong negative correlation still exists when Niño-3.4 leads by 4 months (i.e., Niño-3.4 in May explains about 40% of the September IndoP variance). A similar lead was obtained by Nicholls (1981) using Darwin pressure (as a surrogate for the Southern Oscillation) and Indonesian SST. Closer inspection of Fig. 7a suggests that at shorter leads (1–2 months), similar predictability is implied from IndoT (i.e., local SST) and Niño-3.4 (i.e., Southern Oscillation). But, the correlation at the lag drops off faster for IndoT than for Niño-3.4, so that the implied skill at 3–4 months comes mainly from the knowledge of Niño-3.4. This view is consistent with the notion that IndoT is responding to El Niño conditions in the Pacific. Additional study of this implied predictability is in order, because rainfall anomalies at the end of the dry season appear to have a profound impact in this region.

Seasonally varying, air–sea interaction in the Indonesian region, as discussed previously by Nicholls (1979) and Hackert and Hastenrath (1986), explains the rapid change of sign of local SSTs in going from the dry season to the wet season. However, a nonlocal view is taken here, whereby remote as well as local SST anomalies act to drive the local wind anomaly, which then feeds back onto the SST anomalies. During the dry season anomalous surface easterlies act to increase the local wind speed, cool the ocean surrounding Indonesia, and further decrease the local rainfall, thereby increasing the easterlies. Once the wet season commences and the climatological surface winds across Indonesia shift from southeasterly to northwesterly, the same easterlies will now reduce the wind speed, acting to damp the initial local cold anomaly and damp the surface easterlies.

Previous observational studies (Klein et al. 1999) and model studies (Venzke et al. 2000; Behera et al. 2000; Lau and Nath 2000) have also indicated a prominent role for surface heat flux forcing of SST variations in the Indian Ocean during ENSO. On the other hand, the wind-forced simulations of the Indian Ocean by Murtugudde and Bussalacchi (1999) and Murtugudde et al. (2000) have indicated a prominent role for ocean dynamics. They envision that the cooling during El Niño in the dry season is driven by alongshore (southeastelies) wind anomalies in the eastern Indian Ocean (e.g., Fig. 5), which promote anomalous upwelling off the coast of Sumatra. The cooling is aided by the Kelvin wave response along the equator, which causes the thermocline to elevate in the east (e.g., Chambers et al. 1999). These processes have also been suggested by Webster et al. (1999) and Saji et al. (1999) as a mech-

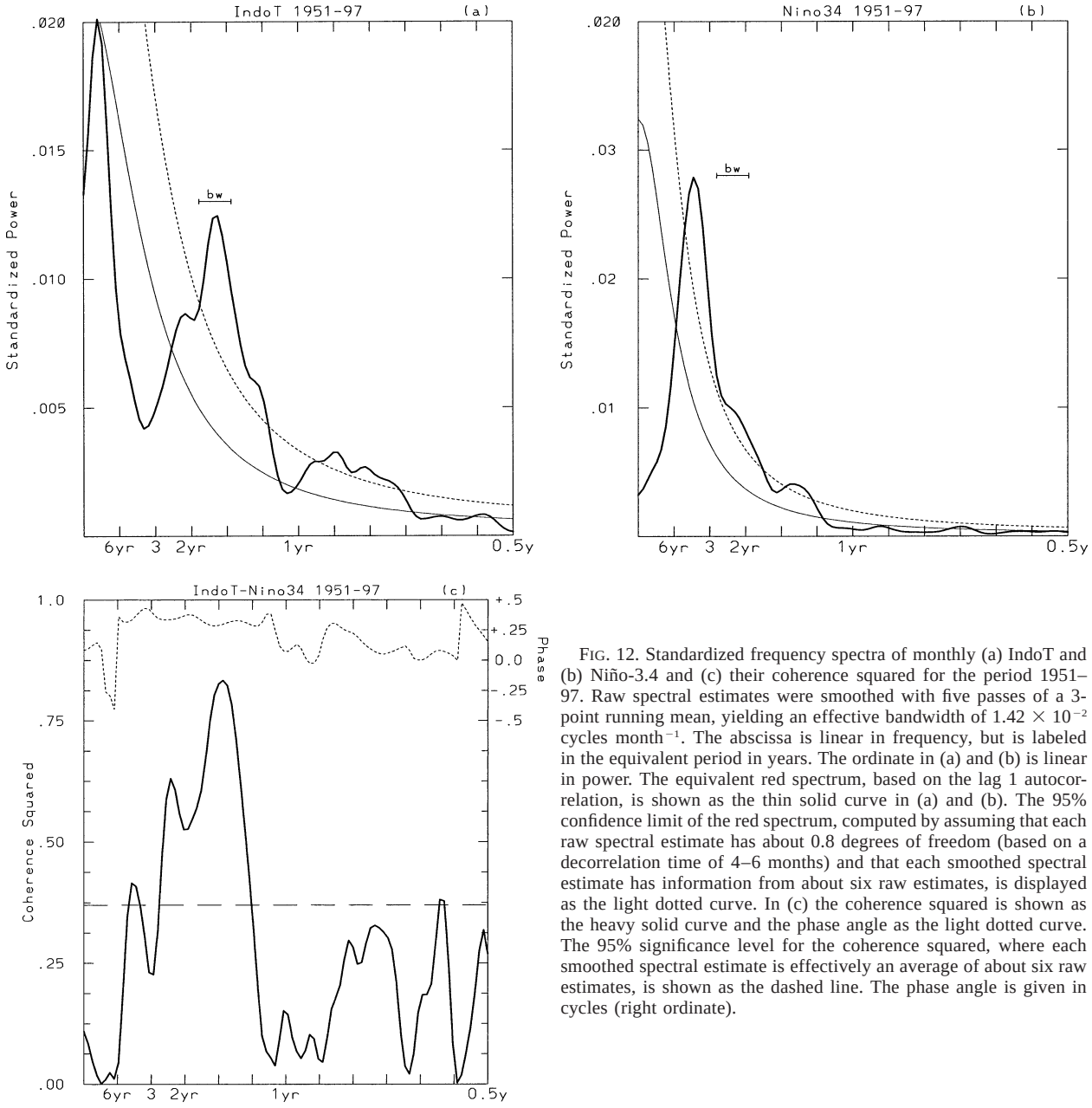

FIG. 12. Standardized frequency spectra of monthly (a) IndoT and (b) Niño-3.4 and (c) their coherence squared for the period 1951–97. Raw spectral estimates were smoothed with five passes of a 3-point running mean, yielding an effective bandwidth of 1.42×10^{-2} cycles month^{-1}. The abscissa is linear in frequency, but is labeled in the equivalent period in years. The ordinate in (a) and (b) is linear in power. The equivalent red spectrum, based on the lag 1 autocorrelation, is shown as the thin solid curve in (a) and (b). The 95% confidence limit of the red spectrum, computed by assuming that each raw spectral estimate has about 0.8 degrees of freedom (based on a decorrelation time of 4–6 months) and that each smoothed spectral estimate has information from about six raw estimates, is displayed as the light dotted curve. In (c) the coherence squared is shown as the heavy solid curve and the phase angle as the light dotted curve. The 95% significance level for the coherence squared, where each smoothed spectral estimate is effectively an average of about six raw estimates, is shown as the dashed line. The phase angle is given in cycles (right ordinate).

anism for coupled behavior in the Indian Ocean that may be excited in the absence of remote forcing by ENSO. A distinction of the SST variability that develops independent of ENSO may be that it is primarily governed by ocean dynamics. The prominent role of surface heat flux forcing associated with ENSO may also be complementary to oceanic dynamical processes (see also Murtugudde et al. 2000 and Baquero-Bernal et al. 2002). Furthermore, it can help account for the initial surface cooling during the development of El Niño that occurs throughout the Indonesian archipelago and well offshore of Sumatra, where upwelling is less effective at promoting cooling (e.g., Murtugudde et al. 2000). The seasonally varying wind–SST feedback also helps explain the rapid surface warming in the eastern Indian Ocean at the onset of the Indonesian wet season, while the surface winds remain southeasterly (i.e., still conducive to coastal upwelling; Fig. 5), the heat content anomalies remain negative, and upwelling and advection still act to cool the eastern Indian Ocean (e.g., Murtugudde et al. 2000).

An unresolved issue is the role that local SST anomalies in the Indonesian region may play in directly driving rainfall anomalies. The present analysis cannot determine which SSTs are predominantly providing the forcing during the dry season, as little independent in-

formation is provided by the local and remote SSTs. And, during the wet season, little correlation between rainfall and local or remote SST is observed. Recent idealized modeling work by Rowell (2001) indicates similar roles for the weaker western Pacific/Indian Ocean SST anomalies and the stronger central/eastern Pacific SST anomalies for driving rainfall anomalies across the Maritime Continent. Additional coupled modeling studies are required to address the issues of local forcing and feedback.

Finally, air–sea interaction in the Indonesian region is postulated to play a fundamental role in generating biennial variations of SST and rainfall. These biennial variations are viewed as a local realization of ENSO (e.g., Rasmusson et al. 1990), whereby anomalous SST in the Pacific drives anomalous winds over the Indonesian region. A biennial SST tendency can be generated if the remotely forced winds are maintained long enough into the wet season in order for the local SST anomalies to change sign. Then, a local feedback between winds and SST can develop in the ensuing dry season. An interesting issue is whether biennial SST variations in the Indonesian region can feed back onto ENSO itself, thus producing the biennial variations in the ENSO cycle that are sometimes observed (e.g., Rasmusson et al. 1990).

Acknowledgments. Support for this work was provided by a CLIVAR Pacific grant from NOAA's Office of Global Programs. John McBride and Malcolm Haylock of BMRC kindly provided the Indonesian station data.

REFERENCES

Baquero-Bernal, A., M. Latif, and S. Legutke, 2002: On dipolelike variability of sea surface temperature in the tropical Indian Ocean. *J. Climate,* **15,** 1358–1368.

Behera, S. K., P. S. Salvekar, and T. Yamagata, 2000: Simulation of interannual SST variability in the tropical Indian Ocean. *J. Climate,* **13,** 3487–3499.

Bergman, J. W., and H. H. Hendon, 2000: Cloud radiative forcing of the low-latitude tropospheric circulation: Linear calculations. *J. Atmos. Sci.,* **57,** 2225–2245.

Bjerknes, J., 1969: Atmospheric teleconnections from the equatorial Pacific. *Mon. Wea. Rev.,* **97,** 163–172.

Chambers, D. P., B. D. Tapley, and R. H. Stewart, 1999: Anomalous warming in the Indian Ocean coincident with El Niño. *J. Geophys. Res.,* **104,** 3035–3047.

Clarke, A. J., X. Liu, and S. Van Gorder, 1998: Dynamics of the biennial oscillation in the equatorial Indian and far western Pacific Oceans. *J. Climate,* **11,** 987–1001.

Deser, C., and J. M. Wallace, 1990: Large-scale atmospheric circulation features of warm and cold episodes in the tropical Pacific. *J. Climate,* **3,** 1254–1281.

Gill, A. E., 1980: Some simple solutions for heat-induced tropical circulations. *Quart. J. Roy. Meteor. Soc.,* **106,** 447–462.

Hackert, E. C., and S. Hastenrath, 1986: Mechanisms of Java rainfall anomalies. *Mon. Wea. Rev.,* **114,** 745–757.

Haylock, M., and J. McBride, 2001: Spatial coherence and predictability of Indonesian wet season rainfall. *J. Climate,* **14,** 3882–3887.

Hendon, H. H., and B. Liebmann, 1990: A composite study of onset of the Australian summer monsoon. *J. Atmos. Sci.,* **47,** 2227–2240.

Kiladis, G. N., and H. F. Diaz, 1989: Global climatic anomalies associated with extremes in the Southern Oscillation. *J. Climate,* **2,** 1069–1090.

Klein, S. A., B. J. Soden, and N.-C. Lau, 1999: Remote sea surface temperature variations during ENSO: Evidence for a tropical atmospheric bridge. *J. Climate,* **12,** 917–932.

Lau, N. C., and M. J. Nath, 2000: Impact of ENSO on the variability of the Asian–Australian monsoons as simulated in GCM experiments. *J. Climate,* **13,** 4287–4308.

Levitus, S., 1982: *Climatological Atlas of the World Ocean.* NOAA Prof. Paper 13, 173 pp. and 17 microfiche.

Meehl, G. A., 1993: A coupled air–sea biennial mechanism in the tropical Indian and Pacific regions: Role of the ocean. *J. Climate,* **6,** 31–41.

Murtugudde, R., and A. J. Bussalacchi, 1999: Interannual variability of the dynamics and thermodynamics of the tropical Indian Ocean. *J. Climate,* **12,** 2300–2326.

——, J. P. McCreary Jr., and A. J. Bussalacchi, 2000: Oceanic processes associated with anomalous events in the Indian Ocean with relevance to 1997–1998. *J. Geophys. Res.,* **105,** 3295–3306.

Newell, R. E., J. W. Kidson, D. G. Vincent, and G. J. Boer, 1974: *The General Circulation of the Tropical Atmosphere.* Vol. 2. The MIT Press, 371 pp.

Nichol, J., 1997: Bioclimatic impacts of the 1994 smoke haze event in Southeast Asia. *Atmos. Environ.,* **31,** 1209–1219.

——, 1998: Smoke haze in Southeast Asia: A predictable recurrence. *Atmos. Environ.,* **32,** 14–15.

Nicholls, N., 1979: A simple air–sea interaction model. *Quart. J. Roy. Meteor. Soc.,* **105,** 93–105.

——, 1981: Air–sea interaction and the possibility of long-range weather prediction in the Indonesian Archipelago. *Mon. Wea. Rev.,* **109,** 2435–2443.

——, 1984: The Southern Oscillation and Indonesian sea surface temperature. *Mon. Wea. Rev.,* **112,** 424–432.

——, and K. K. Wong, 1990: Dependence of rainfall variability on mean rainfall, latitude, and the Southern Oscillation. *J. Climate,* **3,** 163–170.

Rasmusson, E. M., and T. H. Carpenter, 1982: Variations in tropical sea surface temperature and surface wind fields associated with the Southern Oscillation/El Niño. *Mon. Wea. Rev.,* **110,** 354–384.

——, X. Wang, and C. F. Ropelewski, 1990: The biennial component of ENSO variability. *J. Mar. Syst.,* **1,** 71–96.

Ropelewski, C. F., and M. S. Halpert, 1987: Global and regional scale precipitation patterns associated with the El Niño/Southern Oscillation. *Mon. Wea. Rev.,* **115,** 1606–1626.

Rowell, D. P., 2001: Teleconnections between the tropical Pacific and the Sahel. *Quart. J. Roy. Meteor. Soc.,* **127,** 1683–1706.

Saji, N. H., B. N. Goswami, P. N. Vinayachandran, and T. Yamagata, 1999: A dipole mode in the tropical Indian Ocean. *Nature,* **401,** 360–363.

Smith, T. M., R. W. Reynolds, R. E. Livezey, and D. C. Stokes, 1996: Reconstruction of historical sea surface temperatures using empirical orthogonal functions. *J. Climate,* **9,** 1403–1420.

Ting, M., and P. D. Sardeshmukh, 1993: Factors determining the extratropical response to equatorial diabatic heating anomalies. *J. Atmos. Sci.,* **50,** 907–918.

Venzke, S., M. Latif, and A. Villwock, 2000: The coupled GCM ECHO-2. Part II: Indian Ocean response to ENSO. *J. Climate,* **13,** 1371–1383.

Walker, G. T., and E. W. Bliss, 1932: World Weather V. *Mem. Roy. Meteor. Soc.,* **4,** 53–84.

Webster, P. J., A. M. Moore, J. P. Loschnigg, and R. R. Leden, 1999: Coupled ocean–atmosphere dynamics in the Indian Ocean during 1997–98. *Nature,* **401,** 356–360.